# Synthesis and Characterization of Four Consecutive Members of the Five-Member $[Fe_6S_8(PEt_3)_6]^{n+}$ ($n = 0-4$) Cluster Electron Transfer Series

**Christine A. Goddard,† Jeffrey R. Long, and R. H. Holm***

Department of Chemistry, Harvard University, Cambridge, Massachusetts 02138

*Received January 17, 1996*[⊗]

The clusters $[Fe_6S_8(PEt_3)_6]^{+,2+}$ have been shown by other investigators to be formed by the reaction of $[Fe(OH_2)_6]^{2+}$ and $H_2S$, to contain face-capped octahedral $Fe_6S_8$ cores, and to be components of the five-membered electron transfer series $[Fe_6S_8(PEt_3)_6]^{n+}$ ($n = 0-4$) estalished electrochemically. We have prepared two additional series members. Reaction of $[Fe_6S_8(PEt_3)_6]^{2+}$ with iodine in dichloromethane affords $[Fe_6S_8(PEt_3)_6]^{3+}$, isolated as the perchlorate salt (48%). Reduction of $[Fe_6S_8(PEt_3)_6]^{2+}$ with $Na(Ph_2CO)$ in acetonitrile/THF produces the neutral cluster $[Fe_6S_8(PEt_3)_6]$ (65%). The structures of the four clusters with $n = 0$, 1+, 2+, 3+ were determined at 223 K. The compounds $[Fe_6S_8(PEt_3)_6](ClO_4)_3$, $[Fe_6S_8(PEt_3)_6]$ crystallize in trigonal space group $R\bar{3}c$ with $a =$ 21.691(4), 16.951(4) Å, $c = 23.235(6)$, 19.369(4) Å, and $Z = 6$, 3. The compounds $[Fe_6S_8(PEt_3)_6](BF_4)_2$, $[Fe_6S_8(PEt_3)_6](BF_4)\cdot 2MeCN$ were obtained in monoclinic space groups $P2_1/c$, $C2/c$ with $a = 11.673(3)$, 16.371(4) Å, $b = 20.810(5)$, 16.796(4) Å, $c = 12.438(4)$, 23.617(7) Å, $\beta = 96.10(2)$, 97.98(2)°, and $Z = 2$, 4. $[Fe_6S_8(PEt_3)_6](BPh_4)_2$ occurred in trigonal space group $P\bar{1}$ with $a = 11.792(4)$ Å, $b = 14.350(5)$ Å, $c = 15.536(6)$ Å, $\alpha =$ 115.33(3)°, $\beta = 90.34(3)°$, $\gamma = 104.49(3)°$, and $Z = 1$. Changes in metric features across the series are slight but indicate increasing population of antibonding $Fe_6S_8$ core orbitals upon reduction. Zero-field Mössbauer spectra are consistent with this result, isomer shifts increasing by *ca.* 0.05 mm/s for each electron added, and indicate a delocalized electronic structure. Magnetic susceptibility measurements together with previously reported results established the ground states $S = {}^3/_2$ (3+), 3 (2+), ${}^7/_2$ (1+), 3 (0). The clusters $[Fe_6S_8(PEt_3)_6]^{n+}$ possess the structural and electronic features requisite to multisequential electron transfer reactions. This work provides the first example of a cluster type isolated over four consecutive oxidation states. Note is also made of the significance of the $[Fe_6S_8(PEt_3)_6]^{n+}$ cluster type in the development of iron−sulfur−phosphine cluster chemistry.

## Introduction

Over the past decade, a new family of molecular transition metal−chalcogenide clusters of general formulation $[M_6Q_8(PR_3)_6]^{0,z+}$ has emerged. Their cores consist of a regular $M_6$ octahedron face-capped by eight chalcogenide atoms Q. This stellated octahedral geometry is isostructural with the repeating cluster units in the Chevrel phases;[1] however, terminal tertiary phosphine ligands isolate the cores, marking these clusters as links between molecular and extended solids. Thus far, a limited but increasing number of clusters in this family have been prepared and include those with the cores $V_6(O)Se_8$,[2] $Cr_6Q_8$ (Q = S,[3a] Se,[3a] Te[3b]), $Mo_6Q_8$ (Q = S,[4] Se[4b]), $W_6S_8$,[5] $Fe_6S_8$,[6−10] and $Co_6Q_8$ (Q = S,[11] Se,[11f,12] Te[13] ).[14,15]

Cluster compounds, including those above, often support multisequential electron transfer reactions.[16,17] Chemically reversible addition or removal of electrons from clusters can result in measurable changes in core dimensions, which in favorable cases can be traced to the nature of the electroactive orbital. Fast electron transfer rates between members of the same electron transfer series are indicative of low reorganiza-

† National Science Foundation Predoctoral Fellow, 1994−1997.

⊗ Abstract published in *Advance ACS Abstracts,* June 15, 1996.

(1) (a) Chevrel, R.; Sergent, M.; Prigent, J. *J. Solid State Chem.* **1971**, *3*, 515. (b) Bars, O.; Guillevic, J.; Grandjean, D. *J. Solid State Chem.* **1973**, *6*, 48. (c) Fischer, O. *Appl. Phys.* **1978**, *16*, 1 and references therein.

(2) Fenske, D.; Grissinger, A.; Loos, M.; Magull, J. *Z. Anorg. Allg. Chem.* **1991**, *598/599*, 121. This structure contains an interstitial O atom at the center of the $V_6$ octahedron.

(3) (a) Tsuge, K.; Imoto, H.; Soito, T. *Bull. Chem. Soc. Jpn.* **1996**, *69*, 627. (b) Hessen, B.; Siegrist, T.; Palstra, T.; Tanzler, S. M.; Steigerwald, M. L. *Inorg. Chem.* **1993**, *32*, 5165.

(4) (a) Saito, T.; Yamamoto, N.; Yamagata, T.; Imoto, H. *J. Am. Chem. Soc.* **1988**, *110*, 1646. (b) Saito, T.; Yamamoto, N.; Nagase, T.; Tsuboi, T.; Kobayashi, K.; Yamagata, T.; Imoto, H.; Unoura, K. *Inorg. Chem.* **1990**, *29*, 764. (c) Hilsensbeck, S. J.; Young, V. G., Jr.; McCarley, R. E. *Inorg. Chem.* **1994**, *33*, 1822.

(5) (a) Saito, T.; Yoshikawa, A.; Yamagata, T.; Imoto, H.; Unoura, K. *Inorg. Chem.* **1989**, *28*, 3588. (b) Zhang, X.; McCarley, R. E. *Inorg. Chem.* **1995**, *34*, 2678. (c) Ehrlich, G. M.; Warren, C. J.; Vennos, D. A.; Ho, D. M.; Haushalter, R. C.; DiSalvo, F. J. *Inorg. Chem.* **1995**, *34*, 4454.

(6) (a) Cecconi, F.; Ghilardi, C. A.; Midollini, S. *J. Chem. Soc., Chem. Commun.* **1981**, 640. (b) Agresti, A.; Bacci, M.; Cecconi, F.; Ghilardi, C. A.; Midollini, S. *Inorg. Chem.* **1985**, *24*, 689.

(7) Cecconi, F.; Ghilardi, C. A.; Midollini, S.; Orlandini, A.; Zanello, P. *J. Chem. Soc., Dalton Trans.* **1987**, 831.

(8) Bencini, A.; Ghilardi, C. A.; Midollini, S.; Orlandini, A.; Russo, U.; Uytterhoeven, M. G.; Zanchini, C. *J. Chem. Soc., Dalton Trans.* **1995**, 963.

(9) Del Giallo, F.; Pieralli, F.; Fiesoli, L.; Spina, G. *Phys. Lett.* **1983**, *96A*, 141.

(10) Bencini, A.; Uytterhoeven, M. G.; Zanchini, C. *Int. J. Quantum Chem.* **1994**, *52*, 903.

(11) (a) Cecconi, F.; Ghilardi, C. A.; Midollini, S.; Orlandini, A. *Inorg. Chim. Acta* **1982**, *64*, L47; **1983**, *76*, L183. (b) Gervasio, G.; Rossetti, R.; Stanghellini, L. *Inorg. Chim. Acta* **1984**, *83*, L9. (c) Fenske, D.; Hachgenei, J.; Ohmer, J. *Angew. Chem., Int. Ed. Engl.* **1985**, *24*, 706. (d) Cecconi, F.; Ghilardi, C. A.; Midollini, S.; Orlandini, A.; Zanello, P. *Polyhedron* **1986**, *12*, 2021. (e) Hong, M.; Huang, Z.; Lei, X.; Wei, G.; Kang, B.; Liu, H. *Inorg. Chim. Acta* **1989**, *159*, 1. (f) Hong, M.; Huang, Z.; Lei, X.; Wei, G.; Kang, B.; Liu, H. *Polyhedron* **1991**, *10*, 927. (g) Diana, E.; Gervasio, G.; Rossetti, R.; Valdemarin, F.; Bor, G.; Stanghellini, P. L. *Inorg. Chem.* **1991**, *30*, 294. (h) Bencini, A.; Ghilardi, C.; Orlandini, A.; Midollini, S.; Zanchini, C. *J. Am. Chem. Soc.* **1992**, *114*, 9898. (i) Bencini, A.; Midollini, S.; Zanchini, C. *Inorg. Chem.* **1992**, *31*, 2132. (j) Jiang, F.; Huang, X.; Cao, R.; Hong, M.; Liu, H. *Acta Crystallogr.* **1995**, *C51*, 1275.

(12) (a) Fenske, D.; Ohmer, J.; Hachgenei, D. *Angew. Chem., Int. Ed. Engl.* **1985**, *24*, 993. (b) Fenske, D.; Ohmer, J.; Merzweiler, K. *Z. Naturforsch.* **1987**, *42B*, 803. (c) Gervasio, G.; Kettle, S. F. A.; Musso, F.; Rossetti, R.; Stanghellini, P. L. *Inorg. Chem.* **1995**, *34*, 298.

(13) Steigerwald, M. L.; Siegrist, T.; Stuczynski, S. M. *Inorg. Chem.* **1991**, *30*, 2257.

S0020-1669(96)00052-3 CCC: $12.00 

tional barriers and attendant small core structural changes. Although many types of clusters are capable of redox behavior, metal−sulfur clusters exhibit a notably rich reversible electron transfer chemistry. Of the various types of $M_6(\mu_3\text{-}Q)_8$ clusters, those with the $Fe_6S_8$ core have an especially pronounced redox propensity. The first example of these clusters, $[Fe_6S_8(PEt_3)_6]^{2+}$, was reported in 1981 by Cecconi *et al.*[7] Thereafter, $[Fe_6S_8(PEt_3)_6]^{+}$ was described;[8] the structures of both clusters have been established by X-ray analysis.[7−9] Cyclic voltammetry of $[Fe_6S_8(PEt_3)_6]^{2+}$ in dichloromethane solution exhibits four chemically reversible redox events over the potential interval −1.0 to +1.4 V[8] (vs SCE), indicating the existence of *five* consecutive oxidation states $[Fe_6S_8(PEt_3)_6]^{n+}$ with $n = 0-4$ in the electron transfer series (1). Of these, salts of $[Fe_6S_8(PEt_3)_6]^{+,2+}$ have been isolated as $BPh_4^-$ and/or $PF_6^-$ salts. Other members of the series have been electrochemically detected but not isolated.

$$[Fe_6S_8(PEt_3)_6]^{4+} \overset{+1.36\ V}{\rightleftharpoons} [Fe_6S_8(PEt_3)_6]^{3+} \overset{+0.80\ V}{\rightleftharpoons} \underset{S = {}^3/_2}{[Fe_6S_8(PEt_3)_6]^{2+}} \overset{+0.06\ V}{\rightleftharpoons} \underset{S = {}^7/_2}{[Fe_6S_8(PEt_3)_6]^{+}} \overset{-1.03\ V}{\rightleftharpoons} \underset{S = 3}{[Fe_6S_8(PEt_3)_6]^{0}} \quad (1)$$

Such extensive redox flexibility must arise from a closely spaced set of electroactive orbitals, a situation supported by Xα−SW MO results which place the highest set of partially occupied orbitals of $[Fe_6S_8(PEt_3)_6]^{2+,+}$ within an interval of *ca.* 1 eV.[10,11] Associated with this orbital spacing are paramagnetic ground states. Magnetic susceptibility measurements at 20−300 K establish an $S = {}^7/_2$ ($\mu_{eff} = 7.7\ \mu_B$) ground state for $[Fe_6S_8(PEt_3)_6](PF_6)$, which can be rationalized by ferromagnetic coupling between six low-spin $Fe^{3+}$ ($S = {}^1/_2$) and one intermediate-spin $Fe^{2+}$ ($S = 1$).[11] The magnetic behavior of the oxidized cluster $[Fe_6S_8(PEt_3)_6]^{2+}$ as its $BPh_4^-$ [7b] and $PF_6^-$ [11] salts is more complicated because of the marked temperature dependence of the magnetic moment. At 100−300 K, $[Fe_6S_8(PEt_3)_6](BPh_4)_2$ follows the Curie−Weiss law with a Curie constant suggestive of an $S = 3$ state if $g \approx 1.7$. The room-temperature magnetic moment of $[Fe_6S_8(PEt_3)_6](PF_6)_2$ is $\mu_{eff} = 6.6\ \mu_B$ and has been attributed to an $S = 4$ ground state arising from the interaction of five low-spin and one intermediate-spin $Fe^{3+}$ ($S = {}^3/_2$). At lower temperatures the magnetic behavior of both compounds is complex and apparently involves a change in cluster spin as all iron atoms become low-spin. The theoretical calculations admit the $S = 4$ and 3 states in the spin manifold of the cluster. Spin states of other clusters in series 1 are considered below.

Pursuant to our general interest in iron−sulfur clusters and their relevance to biological systems as redox centers, we have synthesized and structurally characterized two additional oxidation states in series 1, $[Fe_6S_8(PEt_3)_6]^{0,3+}$. Together with previous results,[7,8,11] this work provides the first example of a cluster type isolated over *four* consecutive oxidation states. We have taken this unusual opportunity to determine core structural parameters at the same temperature as well as Mössbauer spectroscopic and magnetic properties. These results afford an expanded characterization of this, the most extensive electron transfer series in iron−sulfur cluster chemistry.

## Experimental Section

**Preparation of Compounds.** All operations were performed under pure dinitrogen atmosphere, and solvents were distilled and degassed prior to use by standard procedures unless noted otherwise.

**$[Fe_6S_8(PEt_3)_6](BF_4)_2$.** A solution of 2.00 g (5.93 mmol) of $[Fe(OH_2)_6](BF_4)_2$ in 100 mL of THF was treated with 3.50 mL (23.4 mmol) of $PEt_3$ under stirring to afford a cloudy blue-gray mixture. To this mixture was added 0.11 g (1.0 mmol) of solid $Na_2S_2$ followed by 0.226 g (4.92 mmol) of solid $Li_2S$. The resulting brown-black reaction mixture was stirred overnight. A small aliquot was withdrawn and evaporated to dryness, and the residue was dissolved in acetonitrile; the $^1H$ NMR spectrum revealed the "basket" cluster $[Fe_6S_6(PEt_3)_6]^{+}$ [18] as the only soluble cluster product. The solvent was removed *in vacuo*, the black residue was dissolved in a minimal volume of THF (*ca.* 25 mL), and the solution was filtered. To the filtrate was added 0.096 g (3.0 mmol) of elemental sulfur. The reaction mixture became green-black and was stirred overnight. The $^1H$ NMR spectrum of an aliquot treated as before showed that $[Fe_6S_8(PEt_3)_6]^{+}$ was the only soluble cluster species. The mixture was filtered, and the filtrate was allowed to stand overnight in the air. A black crystalline solid was collected by filtration, washed with THF, and dried *in vacuo* to give 0.22 g (15%) of product. $^1H$ NMR (MeCN): $\delta$ −6.70 ($CH_3$), −45.6 ($CH_2$). Anal. Calcd for $C_{36}H_{90}B_2F_8Fe_6P_6S_8$: C, 29.33; H, 6.15; F, 10.33; Fe, 22.73; P, 12.61; S, 17.40. Found: C, 29.36; H, 6.08; F, 10.41; Fe, 22.75; P, 12.74; S, 17.33.

**$[Fe_6S_8(PEt_3)_6](BPh_4)_2$.** This compound was prepared aerobically. A solution of 0.240 g (163 μmol) of $[Fe_6S_8(PEt_3)_6](BF_4)_2$ in a minimal volume of acetonitrile (*ca.* 1.5 mL) was filtered, and 0.111 g (326 μmol) of solid $NaBPh_4$ was added to the filtrate. The black microcrystalline product that formed immediately was collected by filtration, washed with acetonitrile and ether, and dried *in vacuo*. This material was twice recrystallized by diffusion of ether into saturated solutions of dichloromethane to give 0.29 g (91%) of pure black crystalline product. Anal. Calcd for $C_{84}H_{130}B_2Fe_6P_6S_8$: C, 52.03; H, 6.76; Fe, 17.28; P, 9.58; S, 13.23. Found: C, 52.49; H, 6.78; Fe, 17.60; P. 9.63; S, 13.44. This compound has been prepared previously by a somewhat different procedure.[7]

**$[Fe_6S_8(PEt_3)_6](BPh_4)$.** To a solution of 100 mg (51.6 μmol) of $[Fe_6S_8(PEt_3)_6](BPh_4)_2$ in 1 mL of dichloromethane was added 184 μL (54.2 μmol) of a 0.295 M solution of sodium benzophenide in THF. Solvent was removed *in vacuo*, the residue was washed with ether and redissolved in a minimal volume of dichloromethane, and the solution was filtered. Ether was diffused into the filtrate over 48 h, causing the separation of a solid, which was collected, washed with ether, and dried in vacuo to afford 50 mg (60%) of black crystalline product. $^1H$ NMR ($CD_2Cl_2$): $\delta$ −11.4 ($CH_3$), −71.4 ($CH_2$). Anal. Calcd for $C_{60}H_{110}BFe_6P_6S_8$: C, 44.49; H, 6.85; Fe, 20.69; P, 11.47; S, 15.83. Found: C, 44.29; H, 6.74; Fe, 20.61; P, 11.36; S, 15.68.

**$[Fe_6S_8(PEt_3)_6]$.** A 0.295 M solution of sodium benzophenide in THF (*ca.* 400 μL) was added dropwise to a stirred solution of 74.0 mg (50.2 μmol) of $[Fe_6S_8(PEt_3)_6](BF_4)_2$ in 1 mL of acetonitrile until a black solid precipitated and the supernatant became nearly colorless. The solid was collected, washed with acetonitrile and THF, and then extracted with 5 × 5 mL portions of warm toluene. The brown-black solution of the combined extracts was filtered; rapid addition of acetonitrile to the filtrate caused separation of a black powder. This solid was

(14) The $M_6Q_8$ cubic core is not restricted to molecules with terminal phosphine ligation; cores coordinated by other ligand types include $Zr_6(S)S_82$ and $Re_6Q_8$ (Q = S, Se): (a) Long, J. R.; Williamson, A. S.; Holm, R. H. *Angew. Chem., Int. Ed. Engl.* **1995**, *34*, 226. (b) Long, J. R.; McCarty, L. S.; Holm, R. H. *J. Am. Chem. Soc.* **1995**, *118*, 4603.

(15) For a recent comprehensive account of structural aspects of metal−chalcogenide clusters, *cf.*: Dance, I.; Fisher, K. *Prog. Inorg. Chem.* **1994**, *41*, 637.

(16) (a) Geiger, W. E.; Connelly, N. G. *Adv. Organomet. Chem.* **1985**, *24*, 87. (b) Lemoine, P. *Coord. Chem. Rev.* **1982**, *47*, 55; **1988**, *83*, 169. (c) Drake, S. R. *Polyhedron* **1990**, *9*, 455.

(17) (a) Zanello, P. *Coord. Chem. Rev.* **1988**, *86*, 199. (b) Zanello, P. *Coord. Chem. Rev.* **1989**, *87*, 1. (c) Zanello, P. *Struct. Bonding* (*Berlin*) **1992**, *79*, 101. (d) Zanello, P. In *Stereochemistry of Organometallic and Inorganic Compounds*; Zanello, P., Ed.; Elsevier: Amsterdam, 1994; Chapter 2.

(18) Snyder, B. S.; Holm, R. H. *Inorg. Chem.* **1990**, *29*, 274.

**Table 1.** Selected Crystallographic Data[a] for Cluster Oxidation States **1**−**4** and **6**

| | **1** | **2** | **3** | **4** | **6** |
|---|---|---|---|---|---|
| formula | $C_{36}H_{90}Cl_3Fe_6O_{12}P_6S_8$ | $C_{36}H_{90}B_2F_8Fe_6P_6S_8$ | $C_{84}H_{130}B_2Fe_6P_6S_8$ | $C_{40}H_{96}BF_4Fe_6N_2P_6S_8$ | $C_{36}H_{90}Fe_6P_6S_8$ |
| fw | 1598.8 | 1474.1 | 1938.9 | 1469.4 | 1300.5 |
| crystal system | trigonal | monoclinic | triclinic | monoclinic | trigonal |
| space group | $R\bar{3}c$ | $P2_1/c$ | $P\bar{1}$ | $C2/c$ | $R\bar{3}c$ |
| $Z$ | 6 | 2 | 1 | 4 | 3 |
| $a$, Å | 21.691(4) | 11.673(3) | 11.792(4) | 16.371(4) | 16.951(4) |
| $b$, Å | | 20.810(5) | 14.350(5) | 16.796(4) | |
| $c$, Å | 23.235(6) | 12.438(4) | 15.536(6) | 23.617(7) | 19.369(4) |
| α, deg | | | 115.33(3) | | |
| $\beta$, deg | | 96.10(2) | 90.34(3) | 97.98(2) | |
| $\gamma$, deg | | | 104.49(3) | | |
| $V$, Å$^3$ | 9467(4) | 3004(2) | 2281(2) | 6431(3) | 4818(2) |
| $T$, K | 223 | 223 | 223 | 223 | 223 |
| $R^b$ ($R_w^c$), % | 2.51 (2.83) | 4.49 (5.08) | 4.02 (4.08) | 3.92 (4.08) | 3.18 (3.58) |

[a] Obtained with graphite-monochromated Mo Kα ($\lambda = 0.710\ 73$ Å) radiation. [b] $R = \sum||F_o| - |F_c||/\sum|F_o|$. [c] $R_w = \{\sum[w(|F_o| - |F_c|)^2]/\sum[w|F_o|^2]\}^{1/2}$.

collected by filtration, washed with acetonitrile, and dried *in vacuo* to afford 42 mg (65%) of pure product as a black solid. $^1$H NMR ($C_6D_6$): $\delta$ −6.20 ($CH_3$), −42.0 ($CH_2$). Anal. Calcd for $C_{36}H_{90}Fe_6P_8S_6$: C, 33.25; H, 6.98; Fe, 25.77; P, 14.29; S, 19.72. Found: C, 33.41; H, 6.86; Fe, 25.85; P, 14.19; S, 19.60.

**$[Fe_6S_8(PEt_3)_6](ClO_4)_3$.** This preparation was performed in air. To a solution of 111 mg (75.4 $\mu$mol) of $[Fe_6S_8(PEt_3)_6](BF_4)_2$ in 5 mL of dichloromethane was added a large excess of solid iodine (*ca*. 160 mg, 0.63 mmol). The reaction mixture was stirred overnight, solvent was removed *in vacuo*, and excess iodine was removed from the residue by multiple washings with ether. The residue was redissolved in 20 mL of acetonitrile, and 14.6 mg (75.0 $\mu$mol) of solid $AgBF_4$ was added with stirring to replace the iodide generated in the oxidation reaction with tetrafluoroborate. A light yellow solid (AgI) was removed by filtration. The filtrate was treated with 27.7 mg (226 $\mu$mol) of $NaClO_4$ and refiltered. Several volume equivalents of ether were diffused into the dark solution over 48 h, resulting in the precipitation of black crystals and a white impurity. The solid mixture was collected and washed several times with acetonitrile/THF (1:1 v/v), causing dissolution of the white solid. The remaining solid was dried in vacuo to give the product as 58 mg (48%) of black crystals. $^1$H NMR (MeCN): $\delta$ −2.15 ($CH_3$), −21.1 ($CH_2$). *Anal*. Calcd. for $C_{36}H_{90}Cl_3Fe_6O_{12}P_6S_8$: C, 27.04; H, 5.67; Cl, 6.65; Fe, 20.96; P, 11.62; S, 16.04. Found: C, 26.87; H, 5.62; Cl, 6.58; Fe, 20.83; P, 11.68; S, 16.18.

The compounds of primary interest are now designated as follows:

| | |
|---|---|
| $[Fe_6S_8(PEt_3)_6](ClO_4)_3$ | **1** |
| $[Fe_6S_8(PEt_3)_6](BF_4)_2$ | **2** |
| $[Fe_6S_8(PEt_3)_6](BPh_4)_2$ | **3** |
| $[Fe_6S_8(PEt_3)_6](BF_4)\cdot 2MeCN$ | **4** |
| $[Fe_6S_8(PEt_3)_6](BPh_4)$ | **5** |
| $[Fe_6S_8(PEt_3)_6]$ | **6** |

**X-ray Data Collection and Reduction.** The structures of the five compounds in Table 1 were determined. Crystals of **1**−**3** were grown by vapor diffusion of ether into saturated solutions of acetonitrile (**1**, **2**) and dichloromethane (**3**). In the case of **4**, crystals were obtained by vapor diffusion of ether into a saturated acetonitrile solution of **2** which initially was treated with excess zinc powder prior to diffusion. Crystals of **6** were produced by vapor diffusion of ether into a saturated toluene solution. Crystals were coated with grease, transferred to a Nicolet R3m/V diffractometer, and cooled in a stream of dinitrogen. Lattice parameters were obtained by least-squares analyses of more than 30 carefully centered reflections in the range $10° \le 2\theta \le 30°$. None of the crystals showed significant decay over the period of data collections. Using the program XDISK from the SHELXTL PLUS 4.21/V program package, raw intensity data were corrected for scan speed, background, and Lorentz and polarization effects. An empirical absorption correction was applied to each data set by the program XEMP and observed variations in azimuthal ($\psi$) scans. Crystal data are collected in Table 1. As previously determined at room temperature,[7] compound **3** crystallizes in triclinic space group $P\bar{1}$.

**Structure Solution and Refinement.** Structures of **1**−**4** and **6** were solved by direct methods with the aid of subsequent difference Fourier maps. All structures were refined by full-matrix least-squares and Fourier techniques (XLS). Unless otherwise noted, all non-hydrogen atoms were refined with anisotropic thermal parameters. Hydrogen atoms were given idealized locations with uniform values of $U_{iso}$. The asymmetric units of **1** and **6** consist of one iron atom, two sulfur atoms, one triethylphosphine, and one perchlorate (**1**). The clusters of both **1** and **6** reside on a $\bar{3}$ symmetry site with atom S(2) lying along the 3-fold rotation axis. The perchlorate anion of **1** is severely disordered, requiring the oxygen atom to be refined isotropically over multiple sites with fractional occupancies. For compounds **2** and **3**, the cluster cation is located on an inversion center; three iron atoms, four sulfur atoms, three triethylphosphines, and one anion comprise the asymmetric unit. The tetrafluoroborate anion of **2** was refined isotropically and is disordered with each fluorine atom half-occupying two sites. The asymmetric unit in **4** contains one cluster cation, one anion, and two solvate molecules. Both solvate molecules were refined isotropically. For all structures, difference Fourier maps showed no other electron density, and all parameters shifted by <1% of their esd in the last stages of refinement. Final $R$ factors are given in Table 1.[19]

**Other Physical Measurements.** All measurements were performed under anaerobic conditions. $^1$H NMR spectra were recorded with a Bruker AM-500N spectrometer. Magnetic data were collected on a Quantum Design SQUID magnetometer at fields of 1, 5, and 10 kG. Mössbauer spectroscopic measurements were made and data analyzed with the equipment and procedures described elsewhere.[20] Isomer shifts are referenced to iron metal at room temperature.

## Results and Discussion

**Cluster Synthesis.** Methods for preparation of members of the cluster series $[Fe_6S_8(PEt_3)_6]^{n+}$ ($n = 0-4$) are outlined in Figure 1. The dication $[Fe_6S_8(PEt_3)_6]^{2+}$ was prepared in three steps: self-assembly, oxidative core conversion, and oxidation. The first step involved modified self-assembly of the basket cluster $[Fe_6S_6(PEt_3)_6]^{+}$.[18] Because isolation of this cluster as the $BF_4^-$ salt occurs in low yield,[18] the cluster was used *in situ* after verification of its formation by $^1$H NMR. As previously reported,[18] reaction of the cluster with elemental sulfur affords $[Fe_6S_8(PEt_3)_6]^{+}$. Excess sulfur was used in this step because of the probable competitive reaction with excess triethylphosphine. Formation of the monocation *in situ* was established by NMR; oxidation of this species with dioxygen in THF resulted in crystallization of sparingly soluble **2.** The low yield arises

(19) See paragraph at the end of this article concerning Supporting Information available.

(20) MacDonnell, F. M.; Ruhlandt-Senge, K.; Ellison, J. J.; Holm, R. H.; Power, P. P. *Inorg. Chem.* **1995**, *34*, 1815.

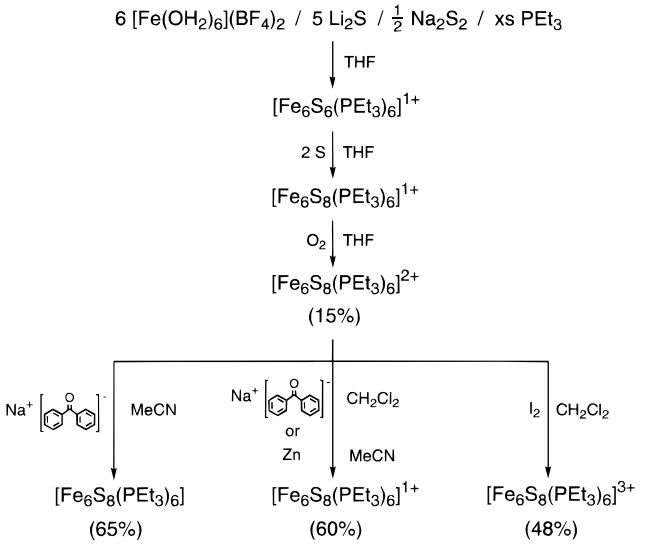


**Figure 1.** Outline of the preparative routes affording the clusters $[Fe_6S_8(PEt_3)_6]^{n+}$ ($n = 0-4$). The $n = 1+$ and $2+$ species have been prepared previously by different methods.[6-8]

from formation of insoluble iron compounds in the first two steps; it is comparable to that (20%) from the reaction of $[Fe(OH_2)_6]^{2+}$, triethylphosphine, and $H_2S$ followed by aerial oxidation, where the cluster was isolated as the $BPh_4^-$ [6] and $PF_6^-$ [8] salts. Compound **2** was readily metathesized to **3** by reaction with $NaBPh_4$ in acetonitrile in high yield (91%).

Reaction of $[Fe_6S_8(PEt_3)_6]^{2+}$ with 1 equiv of $Na(Ph_2CO)$ in dichloromethane solution gave $[Fe_6S_8(PEt_3)_6]^+$, most conveniently isolated as compound **5** (60%). The analogous reaction in acetonitrile with 2 equiv of reductant results in immediate precipitation of neutral cluster **6** (65%). This compound is soluble in warm benzene or toluene and is purified by dissolution in these solvents and precipitation with acetonitrile. Oxidation of $[Fe_6S_8(PEt_3)_6]^{2+}$ with iodine in dichloromethane solution generates $[Fe_6S_8(PEt_3)_6]^{3+}$, which can be crystallized as compound **1** (45%) after removal of iodide (as AgI) and subsequent addition of $NaClO_4$. In series 1, clusters with $[Fe_6S_8]^{0,4+}$ cores have been described as "short-lived".[8,11] This is certainly the expectation for the fully oxidized core which, while reversibly formed in cyclic voltammetry at scan rates >0.1 V/s, is produced at a demandingly positive potential. We have found that fully reduced cluster **6**, while extremely sensitive to oxidation, can be isolated and maintained in solution under anaerobic conditions.

**Structures.** With four consecutive members of series 1 in hand, we have sought detailed structural comparisons by determining all structures at 223 K. As noted earlier, the structures of $[Fe_6S_8(PEt_3)_6]^{2+,+}$ have been determined with $BPh_4^-$ or $PF_6^-$ counterions.[7-9] All crystal structures reported here are new with the exception of **3**. Full metric results for **1** and **6**, containing the accessible fully reduced and oxidized members of the series, are set out in Table 2. Data for the remaining compounds are presented in terms of ranges and mean values in Table 3. All $[Fe_6S_8(PEt_3)_6]^{n+}$ clusters possess the generic $M_6Q_8$ core structure of idealized $O_h$ symmetry illustrated in Figure 2 for $[Fe_6S_8(PEt_3)_6]^{3+}$.

Over the structures of the $n = 0-3$ clusters, the core is composed of a slightly distorted $Fe_6$ octahedron whose faces are capped by $\mu_3$-S atoms. A terminal triethylphosphine ligand completes distorted square pyramidal coordination at each Fe atom, which is displaced by mean values of 0.25−0.31 Å from the $S_4$ cube faces in the direction of this ligand. The clusters in **1** and **6** have the crystallographically imposed $S_6$ symmetry

**Table 2.** Selected Interatomic Distances (Å) and Angles (deg) for **1** and **6**

| | **1** | **6** |
|---|---|---|
| Fe−Fe(A) | 2.581(1) | 2.674(1) |
| Fe−Fe(B) | 2.571(1) | 2.658(1) |
| Fe−S(1) | 2.241(1) | 2.247(1) |
| Fe−S(2) | 2.252(1) | 2.269(2) |
| Fe−S(1A) | 2.234(1) | 2.252(1) |
| Fe−S(1B) | 2.238(1) | 2.253(1) |
| Fe−P | 2.296(1) | 2.237(2) |
| Fe(A)−Fe−Fe(B) | 90.0(1) | 90.0(1) |
| Fe(A)−Fe−Fe(C) | 60.0(1) | 60.0(1) |
| Fe(B)−Fe−Fe(C) | 59.9(1) | 59.8(1) |
| Fe(A)−Fe−Fe(D) | 59.9(1) | 59.8(1) |
| Fe(B)−Fe−Fe(D) | 60.3(1) | 60.4(1) |
| Fe(C)−Fe−Fe(D) | 90.0(1) | 90.0(1) |
| S(1)−Fe−Fe(A) | 114.5(1) | 113.4(1) |
| S(2)−Fe−Fe(A) | 55.0(1) | 53.9(1) |
| S(1)−Fe−Fe(B) | 54.9(1) | 53.9(1) |
| S(2)−Fe−Fe(B) | 114.8(1) | 113.5(1) |
| S(1)−Fe−Fe(C) | 114.6(1) | 113.5(1) |
| S(2)−Fe−Fe(C) | 55.0(1) | 53.9(1) |
| S(1)−Fe−Fe(D) | 54.8(1) | 53.6(1) |
| S(2)−Fe−Fe(D) | 114.8(1) | 114.1(1) |
| Fe(A)−Fe−S(1A) | 114.7(1) | 114.0(1) |
| Fe(B)−Fe−S(1A) | 55.1(1) | 53.9(1) |
| Fe(C)−Fe−S(1A) | 54.8(1) | 53.5(1) |
| Fe(D)−Fe−S(1A) | 115.2(1) | 113.3(1) |
| Fe(A)−Fe−S(1B) | 54.7(1) | 53.7(1) |
| Fe(B)−Fe−S(1B) | 115.1(1) | 113.4(1) |
| Fe(C)−Fe−S(1B) | 114.6(1) | 113.3(1) |
| Fe(D)−Fe−S(1B) | 55.0(1) | 53.8(1) |
| Fe−S(1)−Fe(B) | 70.0(1) | 72.4(1) |
| Fe−S(1)−Fe(D) | 70.1(1) | 72.9(1) |
| Fe(B)−S(1)−Fe(D) | 70.5(1) | 72.3(1) |
| Fe−S(2)−Fe(A) | 69.9(1) | 72.2(1) |
| S(1)−Fe−S(2) | 167.3(1) | 164.5(1) |
| S(1)−Fe−S(1A) | 89.7(1) | 89.4(1) |
| S(2)−Fe−S(1A) | 89.0(1) | 88.6(1) |
| S(1)−Fe−S(1B) | 89.6(1) | 89.3(1) |
| S(2)−Fe−S(1B) | 88.9(1) | 88.5(1) |
| S(1A)−Fe−S(1B) | 167.5(1) | 164.3(1) |
| P−Fe−Fe(A) | 140.6(1) | 137.6(1) |
| P−Fe−Fe(B) | 129.3(1) | 132.4(1) |
| P−Fe−Fe(C) | 136.4(1) | 135.3(1) |
| P−Fe−Fe(D) | 133.0(1) | 134.5(1) |
| S(1)−Fe−P | 91.4(1) | 95.5(1) |
| S(2)−Fe−P | 101.3(1) | 99.2(1) |
| P−Fe−S(1A) | 93.4(1) | 99.9(1) |
| P−Fe−S(1B) | 99.1(1) | 96.5(1) |

illustrated in Figure 3; here the cores approach $D_{3d}$ more closely than $O_h$ symmetry, with the $Fe_6$ octahedra minimally distorted. On the basis of the Fe−Fe(A,B) distances (Table 2), there is a suggestion of a slight compression along the $C_3$ axis. Structural parameters for **2**−**4** at 223 K show no unexpected variation from those of $[Fe_6S_8(PEt_3)_6]X_2$ (X = $BPh_4^-$,[6] $PF_6^-$ [8]) and $[Fe_6S_8(PEt_3)_6](PF_6)$[7] determined at room temperature. Furthermore, mean bond lengths and angles of isoelectronic clusters, isolated as different salts, correlate well under idealized $O_h$ symmetry although some variability of individual core distortions is evident. The $Fe_6$ octahedron in **3** is slightly elongated along the idealized $C_3$ axis, as made evident by the relatively large range in Fe−Fe distances (0.04 Å, Table 3). This result is reinforced by the nearly identical room-temperature structure.[6b] Conversely, the structures of $[Fe_6S_8(PEt_3)_6]^{2+}$ as the $BF_4$- (**2**) and $PF_6^-$ [8] salts display little distortion.

Although structural parameters do not present large variances between clusters, there are distinct trends over the $n = 0-3$ series (Table 3). Proceeding from 29 ($n = 3$, **1**) to 32 (n = 0, **6**) metal-based valence electrons, the mean Fe−Fe bond lengths steadily increase from 2.576(5) to 2.666(8) Å, a total change of 0.09 Å. Concomitantly, the mean Fe−P distances shorten

**Table 3.** Ranges and Means of Selected Interatomic Distances (Å) and Angles (deg) for **1**−**4** and **6**

| | **1** | **2** | **3** | **4** | **6** |
|---|---|---|---|---|---|
| Fe−Fe | 2.571(1)−2.581(1) | 2.607(3)−2.619(3) | 2.602(2)−2.640(2) | 2.626(2)−2.646(3) | 2.658(1)−2.674(1) |
| mean | 2.576(5) | 2.614(4) | 2.618(15) | 2.634(6) | 2.666(8) |
| Fe−S | 2.234(1)−2.252(1) | 2.231(4)−2.262(4) | 2.240(2)−2.256(2) | 2.225(5)−2.283(4) | 2.247(1)−2.269(2) |
| mean | 2.241(7) | 2.249(9) | 2.249(5) | 2.252(18) | 2.255(8) |
| Fe−P | 2.296(1) | 2.286(5)−2.292(5) | 2.288(3)−2.309(2) | 2.235(4)−2.294(4) | 2.237(2) |
| mean | | 2.290(3) | 2.295(10) | 2.270(19) | |
| Fe−$S_4$[a] | 0.246 | 0.267−0.274 | 0.259−0.290 | 0.256−0.302 | 0.305 |
| mean | | 0.270(3) | 0.271(14) | 0.282(15) | |
| S···S | 3.145−3.156 | 3.151−3.169 | 3.133−3.184 | 3.145−3.173 | 3.153−3.163 |
| mean | 3.151(6) | 3.157(6) | 3.159(16) | 3.160(10) | 3.158(5) |
| Fe−Fe−Fe[b] | 59.9(1)−60.3(1) | 59.8(1)−60.2(1) | 59.1()−60.8(1) | 60.4(1)−59.6(1) | 59.8(1)−60.4(1) |
| mean | 60.0(2) | 60.0(1) | 60.0(5) | 60.0(2) | 60.0(2) |
| Fe−Fe−Fe[c] | 90.0(1) | 89.7(1)−90.3(1) | 89.0(1)−91.0(1) | 90.5(1)−89.5(1) | 90.0(1) |
| mean | | 90.0(2) | 90.0(8) | 90.0(3) | |
| Fe−Fe−S[d] | 54.7(1)−55.1(1) | 53.9(1)−54.8(1) | 53.8(1)−59.8(1) | 53.4(1)−55.2(1) | 53.5(1)−53.9(1) |
| mean | 54.9(1) | 54.5(2) | 54.6(11) | 54.2(5) | 53.8(1) |
| Fe−S−Fe | 69.9(1)−70.5(1) | 70.6(1)−71.5(1) | 70.6(1)−72.1(1) | 70.5(1)−72.8(1) | 72.2(1)−72.9(1) |
| mean | 70.1(2) | 71.1(3) | 71.2(5) | 71.6(6) | 72.5(3) |
| S−Fe−S[e] | 88.9(1)−89.7(1) | 88.8(1)−89.6(2) | 88.1(1)−89.9(1) | 88.2(2)−90.6(2) | 88.5(1)−89.4(1) |
| mean | 89.3(4) | 89.2(3) | 89.2(6) | 89.1(7) | 89.0(4) |
| Fe−Fe−P | 129.3(1)−140.6(1) | 132.3(1)−137.5(1) | 131.8(1)−137.8(1) | 130.6(1)−139.6(1) | 132.4(1)−137.6(1) |
| mean | 134.8(42) | 135.0(18) | 135.0(17) | 135.0(20) | 135.0(19) |
| S−Fe−P | 91.4(1)−101.3(1) | 94.0(2)−99.5(2) | 93.3(1)−101.0(1) | 93.9(2)−100.9(1) | 95.5(1)−99.9(1) |
| mean | 96.3(40) | 96.9(17) | 97.0(18) | 97.2(20) | 97.8(18) |

[a] Iron out-of-plane displacement from sulfur-cube face. [b] Within triangular faces. [c] Within equatorial squares. [d] Within sulfide-capped faces. [e] Between neighboring sulfides.

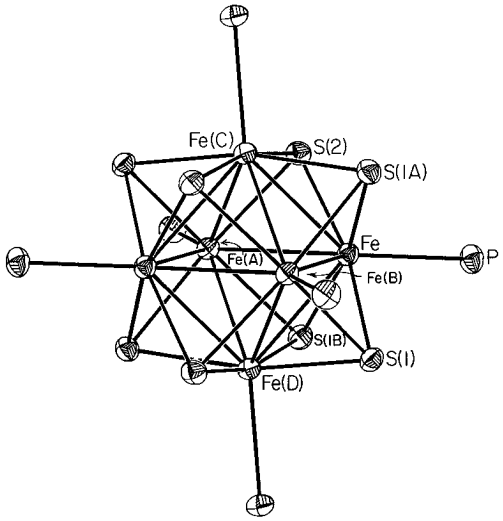


**Figure 2.** Structure of $[Fe_6S_8(PEt_3)_6]^{3+}$ in compound **1**, showing 50% probability ellipsoids and the atom-labeling scheme. Ethyl groups are omitted for clarity.

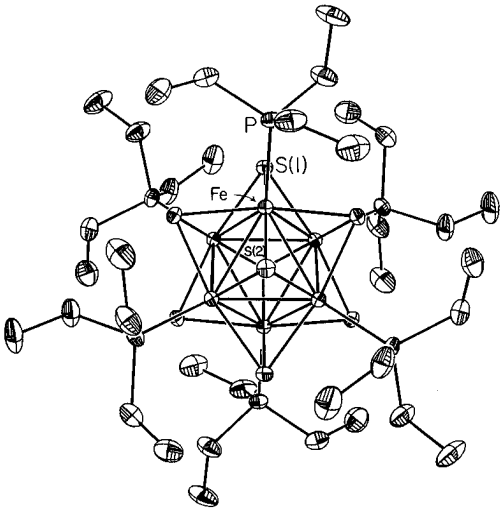


**Figure 3.** Structures of the clusters $[Fe_6S_8(PEt_3)_6]^{n+}$ in compounds **6** ($n = 3$) and **1** ($n = 0$) showing 50% probability ellipsoids, the atom-labeling scheme, and the crystallographically imposed $S_6$ symmetry. The $S_6$ axis is perpendicular to the plane of the plane of the paper.

from 2.296(1) to 2.237(1) Å, a change of 0.06 Å. Mean Fe−S and nonbonded S···S distances do not evidence a statistically significant trend. These results indicate that the core orbitals occupied upon reduction are largely Fe−Fe antibonding, consistent with recent electronic structure calculations.[8] Lengthening Fe−Fe bonds on core reduction results in extension of the $Fe_6$ octahedral vertices farther "outside" the $S_4$ cube faces. Consequently, the mean displacement of the Fe atoms from cube faces monotonically increases from 0.246 to 0.305 Å. As might be expected, increasing core reduction ($Fe^{3.17+} \rightarrow Fe^{2.67+}$, in terms of mean oxidation state) increases the bonding interaction between the iron atoms and the terminal phosphines. The slight changes in Fe−S and S···S distances across the series ($\lesssim$0.01 Å) afford a structural consistency which, together with the small changes in Fe−Fe distances, contribute to the stability and redox flexibility of the $Fe_6S_8$ core.[17a,b]

**Related Clusters.** Mean values of selected structural parameters are collected in Table 4 for comparison with $[Fe_6S_8(PEt_3)_6]^{n+}$ ($n = 0-3$). Similar structure/redox trends are evident in the $Co_6S_8$ clusters, which form the four-membered electron transfer series $[Co_6S_8(PEt_3)_6]^{n+}$ with $n = 0-3$.[11d] Reduction of the $n = 1$ cluster to the neutral species results in an increase of the average Co−Co bond length by 0.023 Å while the average Co−S distance is unchanged. In addition, Co−P bonds correspondingly decrease by 0.024 Å, and the Co atoms move from the $S_4$ core faces as in the $Fe_6S_8$ clusters. In contrast, the core structural changes upon reduction of $[Mo_6S_8(PEt_3)_6]$ to $[Mo_6S_8(PEt_3)_6]^-$ are somewhat different. A small increase in *all* core bond lengths (0.01−0.02 Å) is observed, implying that the LUMO is slightly antibonding. Recent MO calculations on $[Mo_6S_8(PH_3)_6]$, predicting a LUMO Mo 4d and S 3p in character with a weak Mo−S antibonding feature,[21] conform to this result.

(21) Imoto, H.; Saito, T.; Adachi, H. *Inorg. Chem.* **1995**, *34*, 2415.

**Table 4.** Mean Bond Distances (Å) and Number of Metal-Based Electrons for $[M_6S_8(PEt_3)_6]$ Clusters[a]

| | mbe[b] | M−M | M−S | M−P | ref |
|---|---|---|---|---|---|
| $[Mo_6S_8(PEt_3)_6]$ | 20 | 2.663(1) | 2.445(4) | 2.527(3)[c] | 4b |
| $[Mo_6S_8(PEt_3)_6]^-$ | 21 | 2.670(4) | 2.458(7) | 2.550(7) | 4b |
| $[W_6S_8(PEt_3)_6)]$[d] | 20 | 2.679(3) | 2.460(11) | 2.520(5) | 5a |
| $[Fe_6S_8(PEt_3)_6]^{3+}$ (**1**) | 29 | 2.576(5) | 2.241(7) | 2.296(1)[c] | this work |
| $[Fe_6S_8(PEt_3)_6]^{2+}$ (**2**) | 30 | 2.614(4) | 2.249(9) | 2.290(3) | this work |
| $[Fe_6S_8(PEt_3)_6]^{2+}$ (**3**) | 30 | 2.618(15) | 2.249(5) | 2.295(10) | this work |
| $[Fe_6S_8(PEt_3)_6]^{2+}$ [e] | 30 | 2.610(3) | 2.243(9) | 2.285(2) | 9 |
| $[Fe_6S_8(PEt_3)_6]^{2+}$ [f] | 30 | 2.617(14) | 2.247(5) | 2.293(8) | 6b |
| $[Fe_6S_8(PEt_3)_6]^{+}$ (**4**) | 31 | 2.634(6) | 2.252(18) | 2.270(19) | this work |
| $[Fe_6S_8(PEt_3)_6]^{+}$ [e] | 31 | 2.636(2)[c] | 2.251(5) | 2.263(3)[c] | 7 |
| $[Fe_6S_8(PEt_3)_6]$ (**6**) | 32 | 2.666(8) | 2.255(8) | 2.237(2)[c] | this work |
| $[Co_6S_8(PEt_3)_6]^{+}$ | 33 | 2.794(10) | 2.234(12) | 2.163(4) | 11d[g] |
| $[Co_6S_8(PEt_3)_6]$ | 34 | 2.817(3) | 2.233(8) | 2.138(2)[c] | 11d |

[a] All structures were determined at room temperature except those reported in this paper (223 K). [b] Number of metal-based valence electrons. [c] Actual value. [d] Mean values calculated over two molecules. [d] $PF_6^-$ salt. [e] $BPh_4^-$ salt. [g] See also ref 11h.

**Table 5.** Zero-Field Mössbauer Parameters for $[Fe_6S_8(PEt_3)_6]^{n+}$ ($n = 0-3$)

| | $T$, K | $\delta$, mm/s | $\Delta E_Q$, mm/s | $\Gamma$,[a] mm/s |
|---|---|---|---|---|
| $[Fe_6S_8(PEt_3)_6](ClO_4)_3$ (**1**) | 77 | 0.21 | 0.38 | 0.34 |
| | 4.2 | 0.22 | 0.43 | 0.47 |
| $[Fe_6S_8(PEt_3)_6](BF_4)_2$ (**2**) | 77 | 0.26 | 0.33 | 0.30 |
| | 4.2 | 0.26 | 0.27 | 0.40 |
| $[Fe_6S_8(PEt_3)_6](BPh_4)$ (**5**) | 77 | 0.32 | 0.20 | 1.16 |
| | 4.2 | 0.31 | ∼0[b] | 1.58 |
| $[Fe_6S_8(PEt_3)_6]$ (**6**) | 77 | 0.35 | 0.20 | 0.33 |
| | 4.2 | 0.36 | 0.23 | 0.40 |
| $[Fe_6S_8(PEt_3)_6](BPh_4)_2$[c] | 76 | 0.27 | 0.31 | 0.23 |
| | 7 | 0.28 | 0.27 | 0.25 |
| $[Fe_6S_8(PEt_3)_6](PF_6)$[d] | 80 | 0.29 | 0.35 | 0.50 |
| | 5 | 0.28 | 0.32 | 0.36 |
| | | 0.51 | −0.11 | 0.91 |

[a] Line width; fits were constrained such that $\Gamma_R = \Gamma_L$. [b] Spectrum too broad to detect splitting. [c] Reference 9. [d] Reference 8.

**Mössbauer Spectra.** Because all accessible clusters in series 1 with the exception of $[Fe_6S_8(PEt_3)_6]^{2+}$ are mixed-valence, Mössbauer spectra in zero field were determined as one means of examining electron distribution. Parameters from spectral fits are collected in Table 5 and include data for several previously prepared compounds. At 4.2 and 77 K, the spectra consist of a single, essentially symmetric quadrupole doublet, except for that of **5** where the best fit indicated a nil quadrupole splitting. The spectrum of **5** has a substantially broader line width at 77 and 4.2 K, presumably arising from slow or intermediate paramagnetic relaxation. (Because of their simple shapes, the spectra are not presented.) The results for **2** and $[Fe_6S_8(PEt_3)_6](BPh_4)_2$, studied earlier,[9] are in substantial agreement. However, those for **5** and $[Fe_6S_8(PEt_3)_6](PF_6)$ differ in the extent of quadrupole splitting and a six-line hyperfine pattern, which we do not observe with **5**. Lacking more than one detectable iron site, the clusters are considered fully delocalized on the Mössbauer time scale of *ca.* $10^{-7}$ s. Isomer shifts are in or near the normal ranges for Fe(III) and low-spin Fe(II). Their values increase as the core oxidation state decreases, i.e., as the ferrous character increases. The trend is usual but the effect is small, being 0.14 mm/s over the four oxidation states examined here, as might be expected for delocalization over six iron atoms.

We note briefly the parallel behavior of synthetic and native iron−sulfur clusters containing the cores $[Fe_4S_4]^{3+,2+,+}$. In the series $[Fe_4S_4(SR)_4]^{-,2-,3-}$, the isomer shift increases by *ca.* 0.1 mm/s for each electron added.[22−24] In other electron transfer series such as $[Fe_4S_4(S_2C_2(CF_3)_2)_2]^{0,-,2-}$ [25] and $[Fe_4S_4Cp_4]^{2+,+,0}$,[26] the spectra consist of one quadrupole doublet. However, isomer shifts change by ≲0.06 mm/s over the three oxidation states, reflecting substantial ligand character in the electroactive orbital(s). Mössbauer spectra of series $[Fe_4S_5Cp_4]^{2+,+,0}$ have been interpreted in terms of three doublets, one of which remains nearly invariant with oxidation state. Isomer shifts of the other two doublets show an apparent total change of ≲0.1 mm/s, suggesting that three of the four iron atoms are the more directly involved in the redox processes.[27]

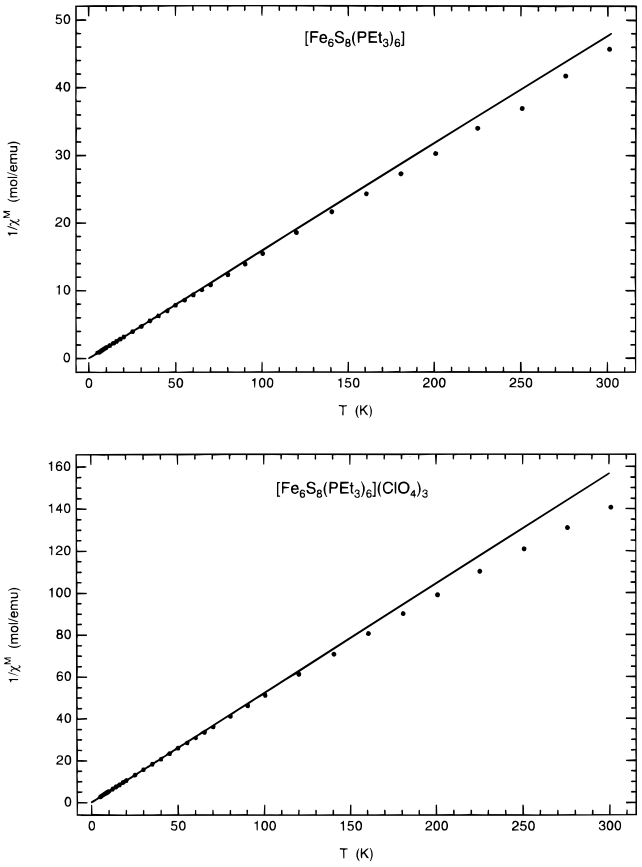


**Figure 4.** Temperature dependencies of the reciprocal molar magnetic susceptibilities of compounds **1** (lower) and **6** (upper) at 1 kG. The lines are fits of the data at 5−20 K to the Curie−Weiss law.

**Magnetic Susceptibilities.** Magnetic data are presented for compounds **1** and **6** as plots of $1/\chi^M$ vs $T$ in Figure 4. Both were measured at applied fields of 1, 5, and 10 kG; the data were fitted to the Curie−Weiss law $\chi^M = C/(T - \Theta)$, which was closely followed by both compounds at all fields at 5−20 K. Average values over the three field strengths are reported in Table 6 together with results for $[Fe_6S_8(PEt_3)_6]^{+,2+}$ compounds.[8,10] Deviations from the Curie−Weiss law at higher temperatures were observed (at all field strengths for **1** and at

(22) Papaefthymiou, V.; Millar, M. M.; Münck, E. *Inorg. Chem.* **1986**, *25*, 3010.
(23) (a) Frankel, R. B.; Averill, B. A.; Holm, R. H. *J. Phys. (Paris)* **1974**, *35*, C6−107. (b) Evans, D. J.; Hills, A.; Hughes, D. L.; Leigh, G. J.; Houlton, A.; Silver, J. *J. Chem. Soc., Dalton Trans.* **1990**, 2735.
(24) (a) Carney, M. J.; Papaethymiou, G. C.; Whitener, M. A.; Spartalian, K.; Frankel, R. B.; Holm, R. H. *Inorg. Chem.* **1988**, *27*, 346. (b) Carney, M. J.; Papaethymiou, G. C.; Spartalian, K.; Frankel, R. B.; Holm, R. H. *J. Am. Chem. Soc.* **1988**, *110*, 6084.
(25) Bernal, I.; Davis, B. R.; Good, M. L.; Chandra, S. *J. Coord. Chem.* **1972**, *2*, 61.
(26) Wong, H.; Sedney, D.; Reiff, W. M.; Frankel, R. B.; Meyer, T. J.; Salmon, D. *Inorg. Chem.* **1978**, *17*, 194.
(27) Dupré, N.; Auric, P.; Hendriks, H. M. J.; Jordanov, J. *Inorg. Chem.* **1986**, *25*, 1391.

**Table 6.** Magnetic Data for Clusters

| compound | *C*,[a] emu K/mol | Θ, K | $\mu_{eff}$, $\mu_B$ | *S* |
|---|---|---|---|---|
| $[Fe_6S_8(PEt_3)_6](ClO_4)_3$[b] (**1**) | 1.93(1) | −0.26(6) | 3.95 | $^3/_2$ |
| $[Fe_6S_8(PEt_3)_6]$[b] (**2**) | 6.30(3) | −0.25(50) | 7.10 | 3 |
| $[Fe_6S_8(PEt_3)_6](PF_6)$[c,e] | | | 7.7 | $^7/_2$ |
| $[Fe_6S_8(PEt_3)_6](PF_6)_2$[d,e] | | | ∼4.3 | 3 |
| $[Fe_6S_8(PEt_3)_6](BPh_4)_2$[f] | 4.662(8) | −20.85(3) | | 3 |

[a] Calculated values with $g = 2$: 1.875 ($S = {}^3/_2$), 6.000 ($S = 3$), 7.875 ($S = {}^7/_2$). [b] Values of C and Θ are averages from measurements at 1, 5, and 10 kG at 5−20 K. [c] 20−300 K. [d] 4.2−20 K; $\mu_{eff} = 4.24\ \mu_B$ for six noninteracting spins. [e] Reference 8. [f] 100−300 K; $C = 4.64$ for $S = 3$ with $g = 1.76$; ref 10.

1 and 5 G for **6**) and are indicative of populated excited states. The Curie constants for **1** and **6** establish the ground states $S = {}^3/_2$ and 3, respectively, provided $g \approx 2$.

The determined ground spin states for compounds **1** and **6** can be rationalized according to previous Xα−SW theoretical results calculated for the model clusters $[M_6S_8(PH_3)_6]^+$ (M = Fe[8], Co[11h]). Because cluster symmetry remains constant and metric features (Table 3) vary little across the oxidation state series, it is reasonable to assume that the relative ordering of MO's would apply to other members of the series. A ground spin state of $S = {}^7/_2$ has been determined previously for $[Fe_6S_8(PEt_3)_6]^+$ and has been qualitatively assigned the electron configuration $(3a_{2g})^1(12e_g + 4a_{2g})^3(12e_u + 4a_{1u})^3$ on the basis of Xα−SW calculations performed under $D_{3d}$ symmetry.[8] Thus, a one-electron reduction should result in either an $S = 4$ state if a higher orbital were occupied or an $S = 3$ state if an electron were added to a half-occupied MO. The $S = 3$ result for **6** is consistent with pairing as would be expected according to the calculated energy gap (1.4 and 1.8 eV for M = Fe and Co, respectively) lying directly above the HOMO. Similarly, one-electron oxidation of $[Fe_6S_8(PEt_3)_6]^+$ is consistent with the $S = 3$ result obtained for $[Fe_6S_8(PEt_3)_6]^{2+}$ at low temperatures and might be expected to have the $(3a_{2g})^1(12e_g + 4a_{2g})^3(12e_u + 4a_{1u})^2$ configuration. The spin state $S = {}^3/_2$ observed for **1** requires spin-pairing, as in the configuration $(3a_{2g})^2(12e_g + 4a_{2g})^3$ or $(12e_g + 4a_{2g})^4(3a_{2g})^1$. Thus, the ground spin states of all isolable clusters in series 1 have been defined, with the proviso that the spin of $[Fe_6S_8(PEt_3)_6]^{2+}$ appears to be dependent on the nature of the anion and attendant intracluster magnetic coupling and crystal structure effects.

**Additional Observations. (a) Redox Capacity.** Few cluster compounds share or surpass the ability of $[Fe_6S_8(PEt_3)_6]^{n+}$ to undergo four reversible one-electron redox events. As one example, the cluster $[Ni_9S_9(PEt_3)_6]^n$ shows four reversible redox reactions ($n = 1-$ to $2+$) but has only been structurally characterized for $n = 2+$.[17a,28] Among Fe−S species, we note the three-membered series $[(MeCp)_4Fe_4S_4]^{0,-,2-}$,[29] the five-membered series $[(MeCp)_4Fe_4S_5]^n$,[30] $[Cp^*_2(Ph_2C_2S_2)_2Fe_4S_4]^n$,[31] and $[Cp^*_3(Ph_2C_2S_2)Fe_4S_5]^n$,[31] and the reversible reduction of the prismatic cluster $[Fe_6S_6(NO)_6]^{2-}$ in four one-electron steps.[32] In nearly all of these cases, the apportionment of electroactive orbitals into metal and ligand contributions is unestablished; dithiolene and nitrosyl ligands are notoriously noninnocent in this context. Series 2 is perhaps most closely related to series

$$[Fe_4S_4(SR)_4]^{4-} \rightleftharpoons [Fe_4S_4(SR)_4]^{3-} \rightleftharpoons [Fe_4S_4(SR)_4]^{2-} \rightleftharpoons [Fe_4S_4(SR)_4]^{-} \quad (2)$$
$$S = {}^1/_2,\ {}^3/_2 \qquad S = 0 \qquad S = {}^1/_2$$

1. Four oxidation states have been detected electrochemically,[33] three of which (3−, 2−, 1−) have been isolated and structurally characterized.[24,34] Potentials of all steps and chemical stabilities of the most oxidized and reduced series members depend upon the R substituent. The entire series is traversed over a potential interval of *ca.* 2 V. Each step of reduction noticeably affects the electron density at the Fe sites (as noted above) and core volumes expand by 2−3%, indicating increasing population of antibonding MO's. Last, $[Fe_6S_8(PEt_3)_6]^{n+}$ clusters embody all the prerequisites necessary and sufficient for substantial redox capacity: relatively high nuclearity and symmetry,[35] contributing to the number and narrow energy spacing of electroactive orbitals with metal character; delocalized electronic structure; an invariant core stereochemistry, abetted by high bridge-atom connectivities ($\mu_{\geq 3}$), affording structural integrity and small Franck−Condon barriers to electron transfer; adequate non-lability of terminal ligands in all core oxidation states. Despite other extensive cluster electron transfer series, $[Fe_6S_8(PEt_3)_6]^{n+}$ clusters, as noted at the outset, are the only ones that have been isolated and structurally characterized in four consecutive oxidation states.

**(b) Iron−Sulfur−Phosphine Clusters.** In addition to the foregoing properties, $[Fe_6S_8(PEt_3)_6]^{n+}$ clusters assume an additional significance. Excluding organometallic compounds, $[Fe_6S_8(PEt_3)_6]^{2+}$, in 1981, was the first Fe−S−$PR_3$ cluster prepared. Prior to that time and thereafter, synthetic Fe−S cluster chemistry has been dominated by investigations of, primarily, $[Fe_2S_2(SR)_4]^{2-}$ and $[Fe_4S_4(SR)_4]^{2-,3-}$ species.[34,36] It has become apparent that inclusion of tertiary phosphines in self-assembly reaction systems, often in weakly polar solvents such as acetonitrile and THF, can direct the synthesis to clusters with different compositions and structures. By such means, the clusters in Figure 5 have been prepared and structurally characterized. Including $[Fe_6S_8(PEt_3)_6]^{n+}$, the group covers six structural types: cuboidal $[Fe_4S_3(NO)_4(PPh_3)_3]$[32] (**7**), cubane-type $[Fe_4S_4(P^tBu_3)_3X]$ (**8**) and $[Fe_4S_4(P^tBu_3)_2(SPh)_2]$[37] (**9**), basket

(28) (a) Ghilardi, C. A.; Midollini, S.; Sacconi, L. *J. Chem. Soc., Chem. Commun.* **1981**, 47. (b) Cecconi, F.; Ghilardi, C. A.; Midollini, S. *Inorg. Chem.* **1983**, *22*, 3802.
(29) Blonk, H. L.; van der Linden, J. G. M.; Steggerda, J. J.; Geleyn, R. P.; Smits, J. M. M.; Beurskens, P. T.; Jordanov, J. *Inorg. Chem.* **1992**, *31*, 957.
(30) Blonk, H. L.; Mesman, J.; van der Linden, J. G. G.; Steggerda, J. J.; Smits, J. M. M.; Beurskens, G.; Beurskens, P. T.; Tonon, C.; Jordanov, J. *Inorg. Chem.* **1992**, *31*, 962.
(31) Inomata, S.; Hitomi, K.; Tobita, H.; Ogino, H. *Inorg. Chim. Acta* **1994**, *229*, 238.
(32) Scott, M. J.; Holm, R. H. *Angew. Chem., Int. Ed. Engl.* **1993**, *32*, 564.
(33) (a) Cambray, J.; Lane, R. W.; Wedd, A. G.; Johnson, R. W.; Holm, R. H. *Inorg. Chem.* **1977**, *16*, 2565. (b) Pickett, C. J. *J. Chem. Soc., Chem. Commun.* **1985**, 323. (c) Weigel, J. A.; Srivastava, K. K. P.; Day, E. P.; Münck, E.; Holm, R. H. *J. Am. Chem. Soc.* **1990**, *112*, 8015.
(34) Berg, J. M.; Holm, R. H. In *Metal Ions in Biology*; Spiro, T. G., Ed.; Interscience: New York, 1982; Vol. 4, Chapter 1.
(35) Among examples of these properties, we note $[Pt_{26}(CO)_{32}]^n$, which has been observed in as many as seven different oxidation states ($n =$ 0 to 6−) coupled by reversible one-electron steps: Roth, J. D.; Lewis, G. J.; Safford, L. K.; Jiang, X.; Dahl, L. F.; Weaver, M. J. *J. Am. Chem. Soc.* **1992**, *114*, 6159.
(36) For a listing of Fe−S clusters built up of edge-sharing tetrahedra (the dominant structural motif in this field), *cf.*: Long, J. R.; Holm, R. H. *J. Am. Chem. Soc.* **1994**, *116*, 9987. Since that time, the cuboidal $[Fe_3S_4(SR)_3]^{3-}$ cluster has been prepared: Zhou, J.; Holm, R. H. *J. Am. Chem. Soc.* **1995**, *117*, 11353. Zhou, J.; Hu, Z.; Münck, E.; Holm, R. H. *J. Am. Chem. Soc.*, in press.
(37) Tyson, M. A.; Demadis, K. D.; Coucouvanis, D. *Inorg. Chem.* **1995**, *34*, 4519.

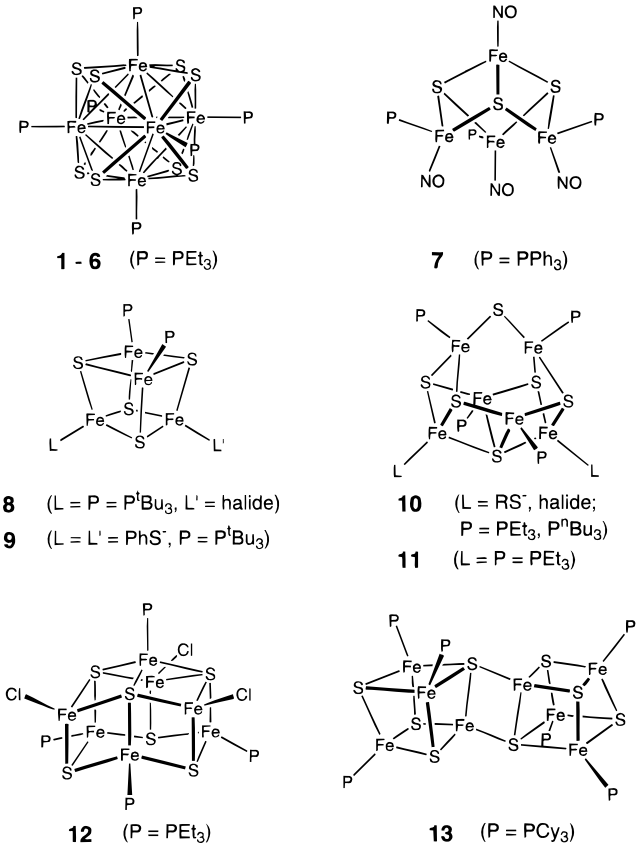


**Figure 5.** Schematic structures of Fe−S−$PR_3$ clusters, including cuboidal **7**,[32] cubanes **8** and **9**,[37] basket clusters **10** and **11**,[18,38] face-capped octahedral clusters found in compounds **1**−**6** and other salts,[6−8] moncapped prismane cluster **12**,[39] and dicubane **13**.[40]

$[Fe_6S_6(PR_3)_4L_2]$[38] (**10**, R = Et, Bu) and $[Fe_6S_6(PEt_3)_6]^{+}$ [18] (**11**), monocapped prismatic $[Fe_7S_6(PEt_3)_4Cl_3]$[39] (**12**), and the dicubane $[Fe_8S_8(PCy_3)_6]$[40] (**13**). All but one cluster are neutral molecules, a probable consequence of the use of low dielectric solvents in synthesis.

As yet, few structural principles are apparent for clusters in Figure 5. We note, however, that, in **10** and **12**, the four and three of the four iron atoms, respectively, terminally ligated by triethylphosphine adopt a trigonal pyramidal $FeS_3P$ arrangement with the metal displaced 0.06−0.15 Å from the $S_3$ plane toward the phosphorus atom. In **12**, the displacement of the unique iron atom is larger (0.37 Å).[39] These values are to be compared with 0.95−0.98 Å displacements of conventional tetrahedral iron atoms with terminal chloride or thiolate ligands in these clusters. While cluster **11** ($[Fe_6S_6(PEt_3)_6]^{+}$) has two tetrahedral iron sites, it is evident that stabilization of trigonal pyramidal sites by $PEt_3$ (cone angle $\theta = 132°$ [41]) is critical to the stability of the cores of **10**−**12**. In this sense, the role of the phosphine bears an apparent similarity to that in $[Fe_6S_8(PEt_3)_6]^{n+}$, with square pyramidal $FeS_4P$ sites and iron atom displacements from $S_4$ planes toward the phosphorus atoms of 0.25−0.31 Å (Table 3). Experiments in this laboratory have indicated that the basket stereochemistry cannot be stabilized with $PCy_3$ ($\theta = 170°$),[41] a result attributed to unacceptable steric interactions between the sulfur atoms and the cyclohexyl groups. Instead, phosphines with very large cone angles appear to force the synthesis of clusters such as **8**, **9**, and **13**, containing ordinary tetrahedral iron sites. For $P^tBu_3$, present in cubanes **8** and **9**, $\theta = 182°$.[41] We consider it unlikely that the cubic $Fe_6S_8$ core will be stabilized by phosphines with such large cone angles. Indeed, Tyson *et al.*[37] consider basket structure **10** incompatible with the cone angle of the $P^tBu_3$ ligand, a view to which we subscribe. Thus, more than in any other facet of iron−sulfur cluster chemistry, it appears that the nature of self-assembled Fe−S−$PR_3$ products is dependent on the steric nature of the terminal ligands. Consequently, new cluster types should emerge upon exploratory synthesis, a matter further confirmed by a current investigation in this laboratory.[42]

**Acknowledgment.** This research was supported by NIH Grant GM 28856. X-ray diffraction equipment was obtained by NIH Grant 1 S10 RR 02247. We thank S. Abedin, Dr. L. Cai, and Dr. M. J. Scott for experimental assistance, Professor G. J. Long for a useful discussion, and Professor C. M. Lieber for use of the SQUID magnetometer.

**Supporting Information Available:** X-ray crystallographic data for the five compounds in Table 1, including tables of data collection and crystal parameters, positional and thermal parameters, and bond angles and distances (58 pages). Ordering information is given on any current masthead page.

IC960052I

(38) (a) Snyder, B. S.; Reynolds, M. S.; Noda, I.; Holm, R. H. *Inorg. Chem.* **1988**, *27*, 595. (b) Snyder, B. S.; Holm, R. H. *Inorg. Chem.* **1988**, *27*, 2339. (c) Reynolds, M. S.; Holm, R. H. *Inorg. Chem.* **1988**, *27*, 4494.

(39) Noda, I.; Snyder, B. S.; Holm, R. H. *Inorg. Chem.* **1986**, *25*, 3851. Displacements of certain Fe atoms from the nearest $S_3$ planes are incorrectly quoted. The correct values are 0.163 Å for Fe(2)−P and 0.968 Å for Fe(3)−Cl.

(40) Cai, L.; Segal, B. M.; Long, J. R.; Scott, M. J.; Holm, R. H. *J. Am. Chem. Soc.* **1995**, *117*, 8863. Cy = cyclohexyl.

(41) Tolman, C. A. *Chem. Rev.* **1977**, *77*, 313.

(42) Goh, C.; Segal, B. M.; Huang, J.; Long, J. R.; Holm, R. H. Submitted for publication.